Chiang Mai J. Sci. 2013; 40(5) : 923-937
http://it.science.cmu.ac.th/ejournal/
Contributed Paper

Microstructural Characterization of Lean Duplex Stainless Steel UNS S32101 Welded Joints Using Electron Backscatter Diffraction

Zbigniew Brytan*[a] and Jerzy Niagaj [b]

[a] Division of Materials Processing Technology, Management and Computer Techniques in Materials Science, Institute of Engineering Materials and Biomaterials, Silesian University of Technology, ul. Konarskiego 18a, 44-100 Gliwice, Poland.

[b] Institute of Welding, ul. Bł. Czesława 16/18, 44-100 Gliwice, Poland.

*Author for correspondence; e-mail: zbigniew.brytan@polsl.pl

Received: 03 July 2012
Accepted: 05 April 2013

Abstract

Microstructural characterization of lean duplex stainless steel UNS S32101 welded joints using scanning electron microscopy (SEM) and electron backscatter diffraction (EBSD) is discussed in the present paper. The influence of isothermal aging heat treatment at 650°C on the microstructures of weld, heat affected zone (HAZ) and parent metal was investigated. The welded joint in the as-welded condition shows Cr_2N nitride precipitation in the HAZ, while isothermal aging at 650°C for 15 min causes further precipitation of nitrides, both in the parent metal, as well as in the HAZ and the weld area. Increasing the aging time at this temperature to 90 min causes the formation of carbides at the grain boundaries and nitride precipitation inside ferritic grains in each zone of the welded joint.

The EBSD analysis of the welded joint after aging at 650°C for 90 min revealed that ferrite content decreased from 45% in parent metal to 40% in HAZ and 39% in the weld. The higher austenite content in the weld, closer to equilibrium, optimized the mechanical properties of welded joints. Grain size of austenite increased gradually from the parent metal over the HAZ to the weld where it was the highest. The ferrite shows smallest grain size in the weld, in the parent metal and the weld it was similar. The orientation relationship between adjacent grains of austenite and ferrite observed from EBSD in the weld metal and the HAZ follows both (K-S) and (N-W) orientation relationship but favors the (N-W) relationship. The presence of such relationship between austenite and ferrite in the weld metal together with the decrease of high-angle grain boundaries in both phases in the welded joint can possibly positively influence the reduction of residual stresses and decrease the susceptibility for crack initiation in the weld metal.

Keywords: EBSD, lean duplex stainless steel, MAG welded joints

1. INTRODUCTION

Stainless steel is the most popular material applied where high corrosion resistance, high surface finish quality, elevated hygienic standards and moderate price are required. The group consists of single phase alloys: austenitic, ferritic, martensitic and precipitation hardening alloys, as well as double phase alloys – duplex stainless steels. The duplex stainless steels combine the properties and advantages of two single phase alloys (ferritic and austenitic) and show higher mechanical properties than the single phase alloys and equivalent or superior corrosion resistance. Duplex stainless steels are less sensitive to stress corrosion cracking than austenitic alloys and show magnetic properties. The duplex stainless steels, based on chemical composition, can be sub-divided into standard duplex, super duplex, hyper duplex and lean duplex stainless steel grades. The standard duplex grades contain 22%Cr, 5%Ni and 3%Mo and the addition of 0.2%N, where the most popular grade is UNS S31803 – designation according to UNS (Unified Numbering System). The next group named super duplex consists of grades with higher alloy content i.e. 25%Cr, 7%Ni and 3-4%Mo, for example grades S32550, S32750, S32760. The latest development includes the new highly alloyed grades called hyper duplex, such as S32707 SAF 2707 HD that contains even higher amounts of alloying elements and the nitrogen content is up to about 0.5%. The high contents of Cr, Mo and N together can give the alloy very high strength and simultaneously good workability for extrusion into seamless tubes used for subsea applications, such as subsea umbilicals to connect platform control stations and wellheads on the seabed [1,2].

In lean duplex stainless steel nickel is partially replaced by manganese. They also contain a high content of nitrogen. In duplex stainless steels Ni, Mn and N stabilize austenite and maintain a balance between austenite and ferrite at about 50%. The use of manganese can ensure proper ferrite-austenite phase balance, while allowing a reduction in nickel content and hence cost. As a result lean duplex stainless steels such as S30403 and S31603 are priced competitively with standard types of austenitic stainless steels - S32101 is the most popular lean duplex stainless steel designed for general-purpose use and like other duplex stainless steels provides both superior mechanical strength and greater chloride stress corrosion cracking resistance compared to austenitic stainless steels - 300 series. A new grade of lean duplex stainless steel was launched in 2010, called LDX 2404® (UNS S82441). This grade contains 3.0% of manganese and 3.6% nickel and has higher chromium and nitrogen contents than standard austenitic grade S31603. Such composition offers higher levels of corrosion resistance making it suitable to withstand the salty atmospheric conditions which prevail in buildings located near the sea. The combination of improved corrosion resistance and high mechanical strength makes UNS S82441 very cost-effective [3].

During the welding of duplex stainless steels the thermal cycle of welding can cause changes in the microstructure not only in the weld material, but also in the heat affected zone. These changes affect both the corrosion resistance of welded joints and their mechanical properties. Sometimes the production cycle involves the heat treatment of welded components or structures made of lean duplex stainless steel. In such situations the additional heating of the welds and heat affected zone can produce carbides, nitrides or sigma phase precipitation – the extent of which depends on the temperature and time of heat treatment. These issues are widely reported in relation to the base material but not when considering welded joints, which may behave differently because they posses initial microstructures that are different from that of the base material depending on the applied welding method, type of filler metal, the amount of heat input [4,5].

Electron Back Scattering Diffraction (EBSD) is a technique based on the analysis of the Kikuchi pattern formed by electron diffraction from individual crystals in specimens in a scanning electron microscope (SEM). The EBSD technique provides quantitative microstructural information about the crystallographic nature of the crystalline materials, where the grain size, grain boundary character, grain orientation, misorientation, texture, phase identity of the sample can be revealed together with statistical measurement and quantitative analysis. Consequently, it has become a very important experimental technique in materials science and engineering [6,7].

The EBSD technique has found a wide field of applications in multiphase materials like duplex stainless steels, where by using this method the nature of ferrite, austenite and any intermetallic phases can be identified. The area fraction and grain size of each phase can also be calculated and the texture in each phase can be identified. This can give detailed information about the thermal and processing history and the mechanical properties of the steel [8-12].

The austenite (γ) can have a specific crystallographic orientation relationship with the ferrite (α) due to phase transformation occurring during the heating and cooling in a duplex stainless steel weld joint. The relationships present in duplex stainless steel between neighboring austenite and ferrite grains are often close to Kurdjumov – Sachs (K-S) $\{111\}\gamma // \{011\}\alpha$, $<011>\gamma // <111>\alpha$ and Nishiyama – Wasserman (N-W) relationships $\{111\}\gamma // \{011\}\alpha$, $<112>\gamma // <011>\alpha$ [13]. These two relationships differ by only with few degrees in rotation in the interface plane between austenite and ferrite, where K-S relationship corresponds to a 42.8° misorientation angle and N-W relationship to 45.9° [14]. The presence of such relationships between austenite and ferrite in the weld metal may have influence on the easier propagation of dislocation slip from one phase to the other and thus reduce the distribution of residual stresses [15] Presence of the K-S relationship between austenite and ferrite was recently connected with lower tendency to microcracks nucleation on the phase boundaries [16].

This paper presents a few examples of SEM and the EBSD analysis applied in the microstructure characterization of different zones of the welded joints of lean duplex stainless steel S32101 after isothermal aging at 650°C.

2. MATERIALS AND METHODS

Lean duplex stainless steel as cold rolled and annealed sheet according to ASTM A240 S32101 (EN 1.4162) with a thickness of 6 mm was used for the study (Table 1). The welding joints were produced using the metal active gas (MAG) method where the filler metal was in wire form grade Avesta LDX 2101 with a diameter of 1.2 mm, as in Table 2. During the process a shielding gas mixture of Ar + 2.5% CO_2 was applied and as a forming gas pure technical argon according to standard EN ISO 14175-I1-Ar was used.

Table 1. Chemical composition of lean duplex stainless steel S32101.

Grade	Sheet thickness, mm	Chemical composition, wt %							
		C	Si	Mn	Cr	Ni	Mo	Cu	N
S32101	6	0.028	0.70	4.90	21.34	1.50	0.19	0.25	0.21

Table 2. Chemical composition of wire electrode, grade AVESTA LDX 2101.

Wire grade	Wire diameter, mm	Chemical composition, wt %									
		C	Si	Mn	P	S	Cr	Mo	Ni	N_2	Cu
AVESTA LDX 2101	1.2	0.016	0.53	0.75	0.029	0.001	23.12	0.25	7.27	0.117	0.17

The welding joints were produced using a mechanized welding stand consisting of a semi-automatic welding machine with synergistic control (Kemppi Pro 5,200), a welding trolley (DC20 PROMOTECH) with precisely adjustable travel speed of torch and an attachment device to position welded pieces. The shielding gas flow during MAG welding was adjusted between 14 and 16 l/min, while the forming gas was set to 5-6 l/min. The welding was carried out using direct current with the positive end of the consumable electrode (DC +). The parameters of MAG welding for butt joints of 6 mm thickness made of lean duplex stainless steel S32101 are summarized in Table 3.

Table 3. The MAG welding parameters of testing butt joints.

Joint symbol	Number of beads	Welding current, A	Arc voltage, V	Welding speed, cm/min	Heat input, kJ/mm
6-20	1	116	22.6	9.2	1.368

After welding the test joints were subjected to heat treatment by aging at temperatures of 650°C for 15 and 90 min. in a neutral atmosphere.

Microstructure observations of welded joints were carried out using light and scanning electron microscopy. Light microscope observations involved etching using Aqua Regia reagent and were performed at 400x and 1,000x magnifications using a LEICA MEF4A microscope. The scanning electron microscope (SEM) involved in the studies was a SUPRA 25 of ZEISS Company equipped with an EDS probe. The SEM Inspect F with EBSD equipped with the automatic OIM (orientation imaging microscopy) software from TSL has been used to obtain more information about grain structure than from optical microscopy. The samples for EBSD analysis were ground, polished with silicon carbide paper from grade 220 to grade 4,000, and then with diamond paste (1 and 0.25 μm) on polishing clothes and finally argon-ion beam polished. The EBSD measurements were performed at 20 keV with a step size of 20 μm. The microstructural analysis was performed in the middle of the welded zone, around the root of weld, heat affected zone (HAZ) and in parent metal (Figure 1).

a) b)

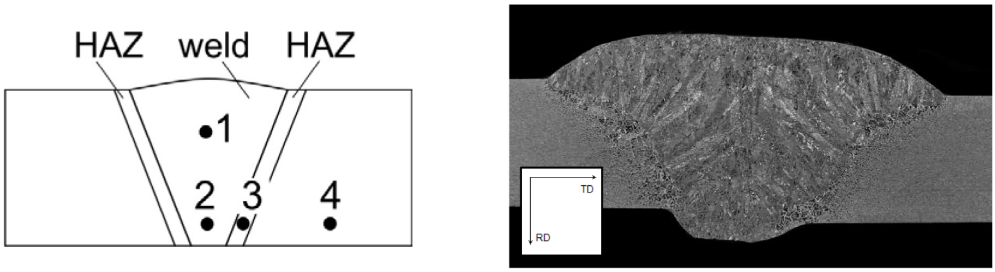

Figure 1. The areas of microstructural studies in the welded joint, a) the arrangement of studied zones, b) cross-sectional photo of studied joint (1 – the weld, middle; 2 – the weld, root; 3 – the heat affected zone HAZ; 4 – the parent metal PM).

During SEM observations the EBSD analysis was applied in three different zones of each welded joint i.e. in the weld, HAZ and the parent metal. Crystal orientation maps (COM) were generated including the distribution of low- and high-angle boundaries, distribution of misorientation angles between all adjacent points, distribution of phases, grain size, grain size aspect ratio (defined as the minor axis of an ellipse divided by its major axis of a fitted ellipse, so a grain with a high aspect ratio has a needle-like shape), inverse pole figures for individual phases and the phase content in individual zones of the welded joint. The EBSD analyses were performed on the plane perpendicular to the welding direction on the transverse section of the weld, where the axis designation for EBSD, the (TD) axis correspond to horizontal direction and (RD) axis correspond to vertical direction (Figure 1b).

3. Experimental Results and Discussion

Microstructural analysis of the individual zones of the welded joints by light microscopy revealed that the weld area contained more austenite than the HAZ and parent material (Figure 2).

The microstructural analysis by SEM confirmed that in the as-welded conditions weld material is characterized by mixed distribution of both phases (ferrite and austenite), where in ferritic matrix the austenite of different shape and orientation precipitated. There are also small areas of intracellular austenite with characteristic trapezoidal and orthorhombic shape (Figure 3a). Secondary phase precipitation has not been observed at grain boundaries of either phase. However in the HAZ, very numerous small precipitates probably of chromium nitride Cr_2N [4, 8-10] were observed in the ferrite grains and in ferrite/ferrite grain boundaries (Figure 3b). This phenomenon occurred only in the HAZ and its range does not exceed beyond this zone. The parent metal microstructure was free of secondary phase precipitation. The microstructure of material in the weld area is characteristic for the welded duplex stainless steels with uneven distribution of both phases. The chemical composition measured with EDS analysis in the weld zone show very uniform distribution of alloying elements, expressed by partial coefficient (α/γ wt%), which for Cr = 1.1 and Mn = 0.81 and Ni= 0.97 indicating

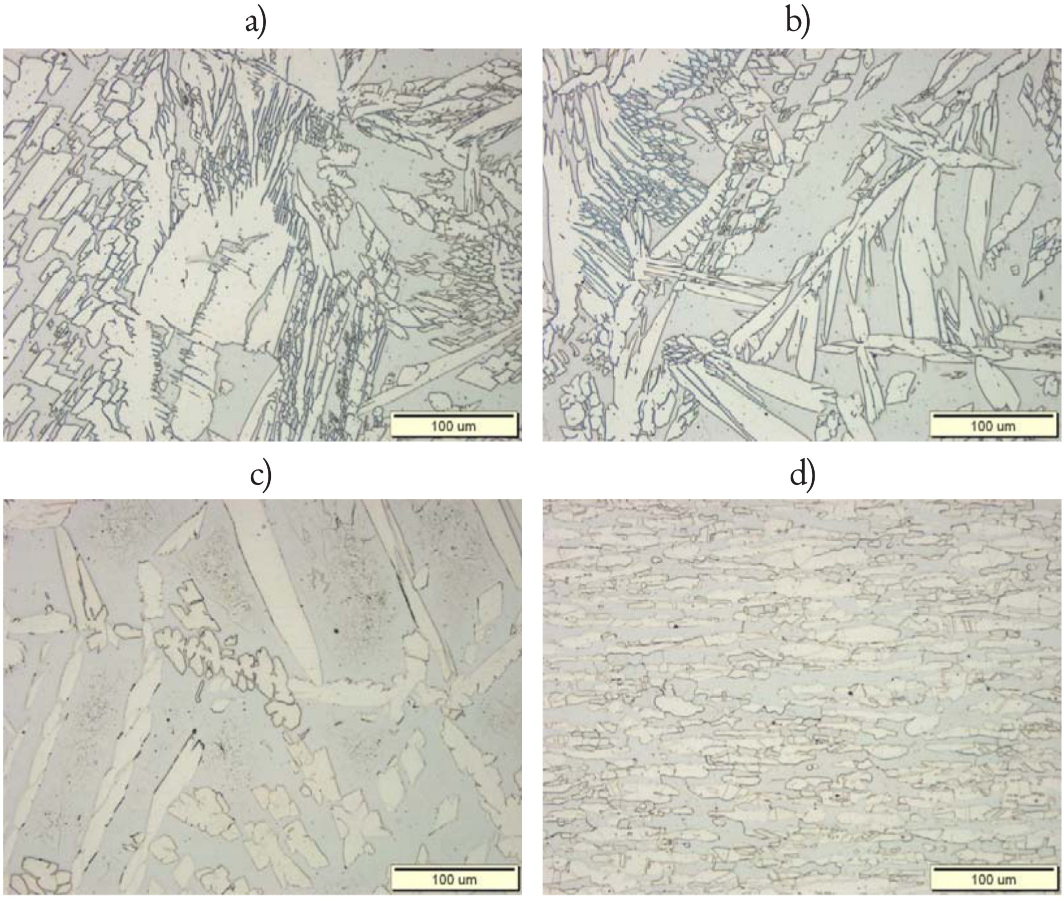

Figure 2. The microstructure in as-welded conditions of lean duplex stainless steel S32101 in various zones, where a) the weld centre (point 1 acc. to Figure 1), b) the weld root (point 2 acc. to Figure 1), c) HAZ (point 3 acc. to Figure 1), d) parent material (point 4 acc. to Figure 1).

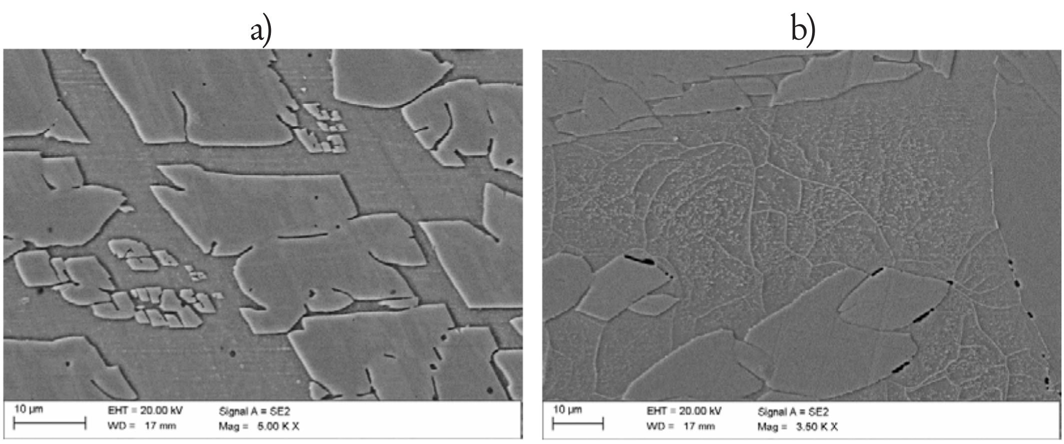

Figure 3. The microstructure of lean duplex stainless steel S32101 of the welded joint in as-welded condition, evaluated by SEM, where a) the weld area and b) the HAZ.

that ferrite (α) is dominated by chromium and austenite (γ) is enriched in nickel and manganese and has lower concentrations of chromium.

The isothermal heat treatment of the welded joint at 650°C for only 15 min results in precipitation of chromium nitrides Cr_2N in the material, both in the weld metal (Figure 4a) and heat affected zone (HAZ) and in the parent metal (Figure 4b). After this heat treatment the presence of carbides at austenite/ferrite grain boundaries was not observed. Extending the holding time in this temperature to 90 min results in the precipitation of the increased amount of nitrides Cr_2N and according to some reports [4, 11] of carbides, probably $M_{23}C_6$ type at the grain boundaries of austenite and ferrite, which occurs in a balanced way in each zone of welded joint - in the weld, HAZ and parent metal. The precipitation of nitrides and carbides after isothermal aging are less harmful to mechanical properties, than precipitation of sigma phase (σ) [12], since its formation can cause rapid deterioration in toughness and corrosion resistance. The formation of sigma phase (σ) occurs when the cooling rate during welding is not fast enough and the more highly alloyed the duplex stainless steel, the higher is the probability of its formation. Therefore, hyper and superduplex steels are more prone to this problem than lean duplex stainless steel.

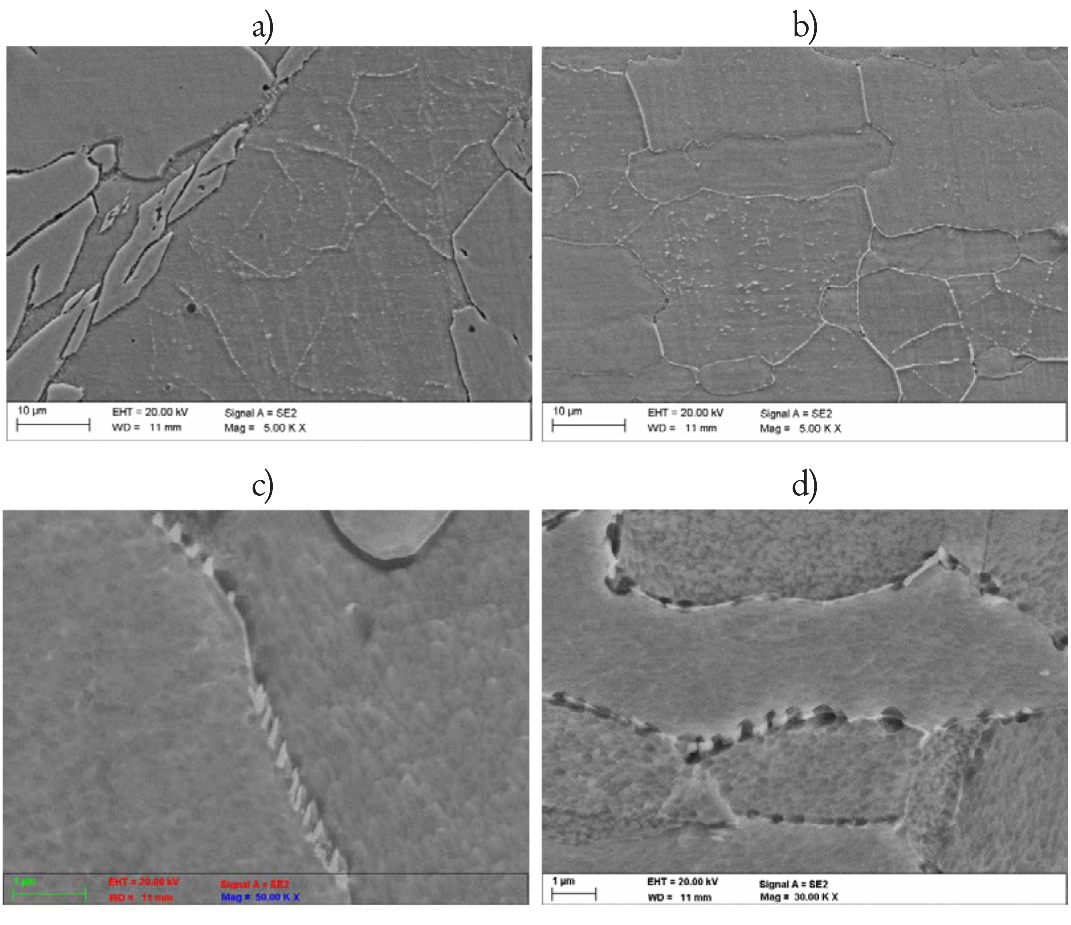

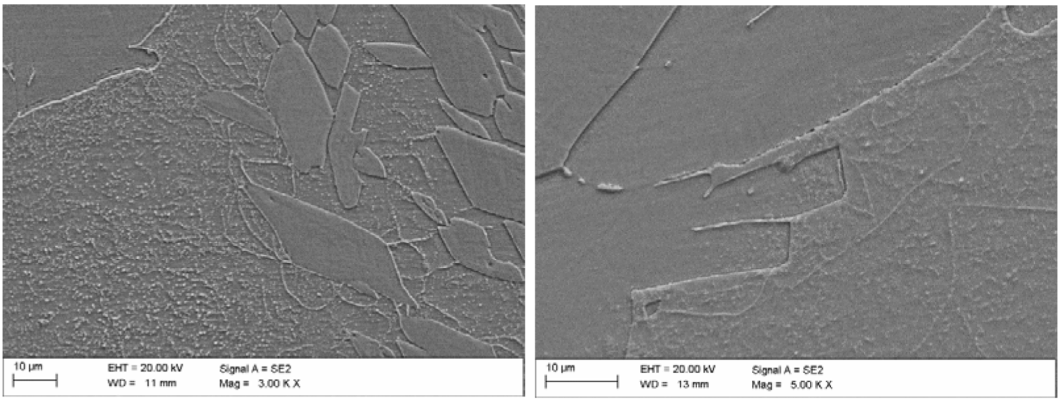

Figure 4. The microstructure of the welded joint after aging at 650°C, a) and b) after aging for 15 min, a) the weld (area 1) and b) the parent metal (area 4), and c) and d) after aging for 90 min, c) the weld and d) the parent metal, e) and f) the HAZ, e) after aging for 15min and f) after aging for 90min.

Detailed EBSD analysis of the sample after aging at 650°C for 90 min was performed (Figure 5-7) to evaluate any differences in the nature of austenite and ferrite in particular zones of welded joints. This condition was selected due to marginal changes in main phase balance, the austenite and ferrite, compared to the as-weld condition and after aging for 15 min. Small precipitates such carbides or nitrides will be analyzed in future work. The phase map in the parent metal (Figure 5) shows the ferrite content in this zone to be 45% with predominated low-angle boundaries, about 84% (the boundaries with misorientation angle between 2° and 15°) of all boundaries present in the ferrite. The inverse pole figure of ferrite shows strong alignment to the <110> axes (Figure 5b). Average grain size diameter of ferrite was calculated as 9.04 μm (7.88 - excluding edge grains), where the equivalent area of fitted ellipse was 64.18 (48.81) μm^2 (Table 4). Average grain shape (excluding edge grains) was calculated by computing the average area and aspect ratio and then using a fitting approach to determine the angle between the major axis to the horizontal. The grain shape was described by the major and minor axis of an equivalent ellipse. The major axis was measured as 10.18 (8.70) μm, and minor axis 3.77 (3.40) μm, where the angle of major axis to the horizontal was 66.18 (70.25) degrees. The austenite phase in the parent metal shows predominantly high-angle boundaries, about 70% (the boundaries with misorientation angle above 15°). The inverse pole figure of austenite shows strong orientation of this phase between <111> and <001> axes. The average grain size of austenite was smaller than that of ferrite. The average grain shape expressed by major axis of equivalent ellipse was 6.16 μm and the minor axis was 2.71μm, smaller than for ferrite. Detailed comparison of the grain size and grain shape of austenite and ferrite in particular zones of the welded joint are summarized in the Table 4. The grain shape aspect ratio of austenite in each zone of the weld was in the range between 0.42 to 0.44, while the grain shape aspect ratio of ferrite was increased from 0.37, characteristic for parent metal to 0.50 in HAZ and 0.46 in the weld area.

Table 4. The grain size and grain shape of austenite and ferrite in particular zones of the welded joint.

Zone of welded joint	Phase	Grain size *		Average grain shape*			
		The average grain size, μm	Equivalent area, μm^2	Major axis, μm	Minor axis, μm	Grain shape aspect ratio	Angle to horizontal, degrees**
Parent metal	α	9.04 (7.88)	64.18 (48.81)	10.18 (8.70)	3.77 (3.40)	0.37 (0.39)	66.18 (70.25)
HAZ		6.91 (5.81)	37.51 (26.50)	9.22 (7.11)	4.64 (3.67)	0.50 (0.51)	356.37 (168.42)
Weld		9.45 (8.19)	70.08 (52.64)	12.67 (9.47)	5.90 (4.54)	0.46 (0.47)	352.20 (163.80)
Parent metal	γ	7.32 (7.31)	42.07 (41.91)	6.16 (6.09)	2.71 (2.74)	0.43 (0.45)	18.04 (15.97)
HAZ		11.99 (11.40)	112.85 (102.09)	14.28 (13.64)	6.40 (6.33)	0.44 (0.46)	358.91 (179.48)
Weld		13.44 (12.36)	141.86 (119.97)	15.99 (13.83)	6.80 (6.09)	0.42 (0.44)	340.11 (158.60)

* Grain size estimated based on the fitted ellipse and its diameter and equivalent area, where the ellipse with minor and major axis represent shape aspect ratio
** Grain shape orientation refers to the angle of the major axis from the horizontal
The values in brackets () refers to values excluding edge grains – excluding points considered as edge grains

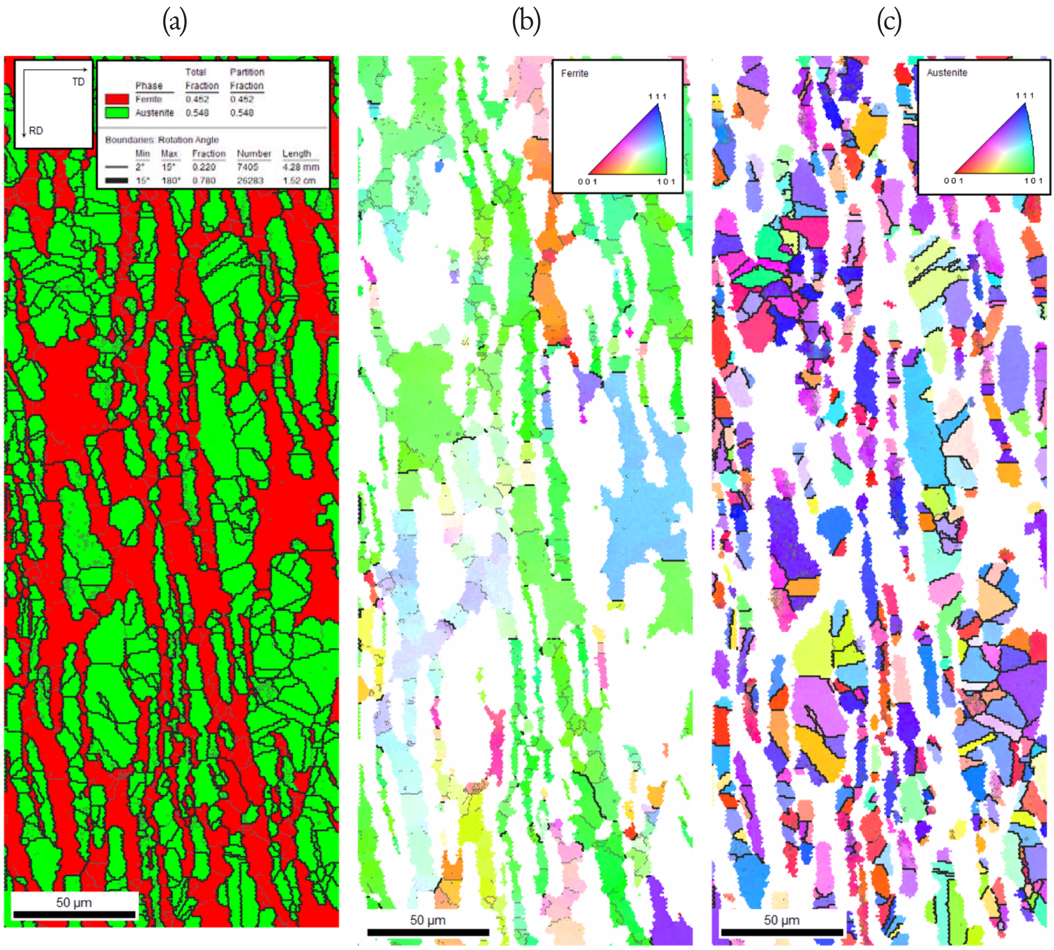

Figure 5. The EBSD maps of the parent metal microstructure, a) phase map and color coded map - inverse pool figure [001] of b) ferrite and c) austenite, the color code for presented microstructures is as follows: the red means a [001] crystal direction, blue a [111] direction, and green a [101] direction, respectively.

The EBSD mapping in the weld zone (Figure 6a) confirmed lower ferrite content in this zone, about 39%, about 93% of the boundaries in the ferrite phase were rated low-angle and 7% high-angle boundaries. Austenite contained both low- and high-angle boundaries, where the number of high-angle boundaries was decreased compared to parent metal and contained 56% of high-angle boundaries. The ferritic phase shows preferential grain orientation according to <001> direction (Figure 6b), while austenite grains shows mixed orientation (Figure 6c). The austenite shows an increase in average grain size and 3x increase of equivalent area of grain size (Table 4).

(a) (b) (c)

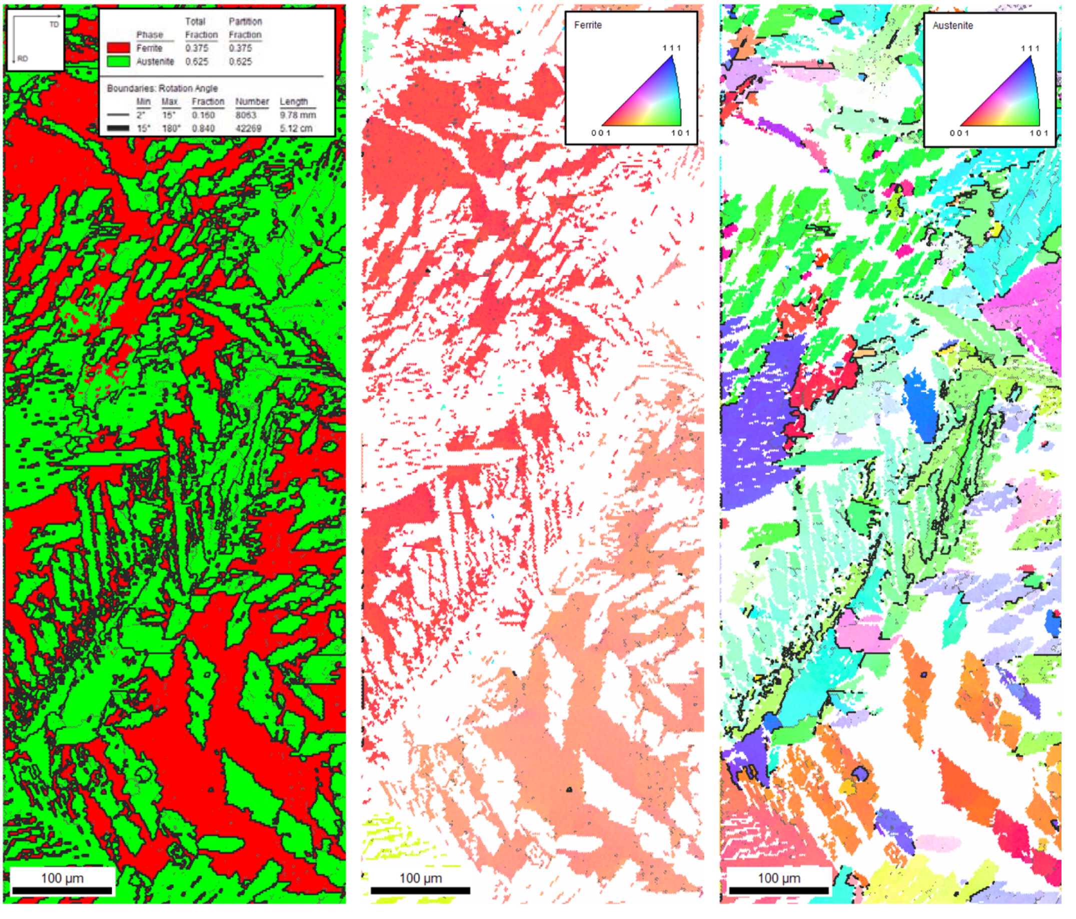

Figure 6. The EBSD maps of the weld microstructure, a) phase map and color coded map - inverse pool figure [001] of b) ferrite and c) austenite, the color code for presented microstructures is as follows: the red means a [001] crystal direction, blue a [111] direction, and green a [101] direction, respectively.

The HAZ shows a ferrite content of 40% (figure 7a). The grain shapes in this zone of the welded joint are more elongated with higher grain shape factor compared to the weld and parent metal (Table 4) and both phases show either low- and high-angle grain boundaries. The ferritic phase (Figure 7b) as well as austenitic (Figure 7c) shows mixed orientation. The respective amounts of high-angle boundaries in ferrite and austenite are 35% and 52%.

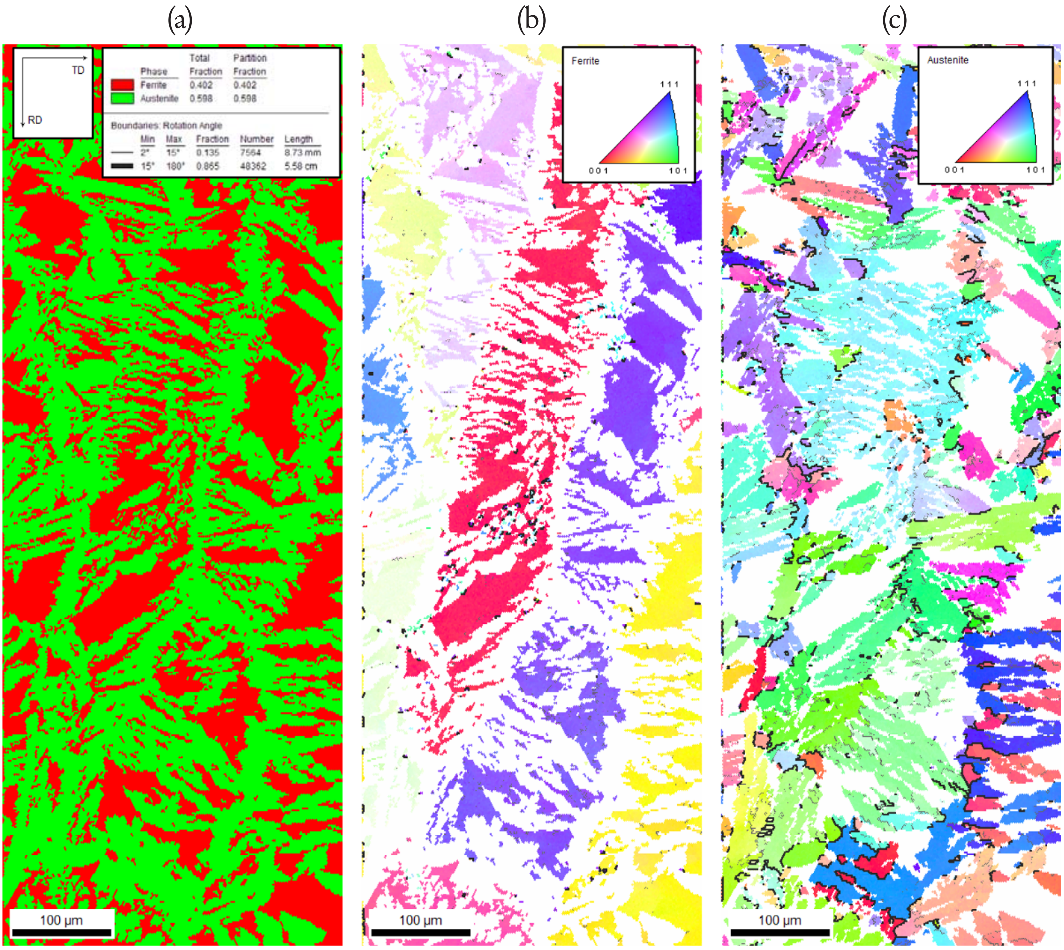

Figure 7. The EBSD maps of the HAZ microstructure, a) phase map and color coded map - inverse pool figure [001] of b) ferrite and c) austenite, the color code for presented microstructures is as follows: the red means a [001] crystal direction, blue a [111] direction, and green a [101] direction, respectively.

Studied lean duplex stainless steel weld metal shows regions of Widmanstatten-type austenite (Figure 6 and 7) typical of a fully ferritic solidification mode that provide a positive influence on the weld impact toughness. The duplex weld metal solidifying completely as ferrite shows generally higher toughness level than structures solidifying in mixed austenitic-ferritic mode [17].

For each EBSD map, the proportions of small (2° - 15°) and large (45° - 180°)

misorientations between all adjacent points were calculated, thus the boundaries with a misorientation angle less than 15° were defined as low angle boundaries and these with an angle greater than 45° were termed as high angle boundaries. Figure 8 shows the distribution of the misorientation angle between austenite and ferrite boundaries for each studied zone. The misorientation angle between austenite and ferrite boundaries in the parent material lies preferentially near low angles below 5° and gradually increases near 40-45° and shows random misorientation angle distribution (Figure 8a). The average grain misorientation angle in the weld and also in the HAZ between phases of lean duplex stainless steel welded joint lies near 40-45°, which contains both Nishiyama-Wassermann (N-W) and Kurdjumov-Sachs (K-S) crystallographic orientation relationships (Figure 8b and 8c). The austenite phase can precipitate with near (N-W) or (K-S) orientation relationship. This result agrees with earlier results from the literature [18]. The (K-S) orientation relationships correspond to a 42.8° misorientation angle and (N-W) relationship to 45.9° so detailed analysis in this range was performed. This indicates that the orientation relationship between austenite and ferrite in the studied lean duplex stainless steel weld metal and HAZ is closer to the (N-W) orientation relationship than to the (K-S) one. The HAZ shows even slightly higher number of analyzed fractions that follows (N-W) orientation relationship than that in the weld zone.

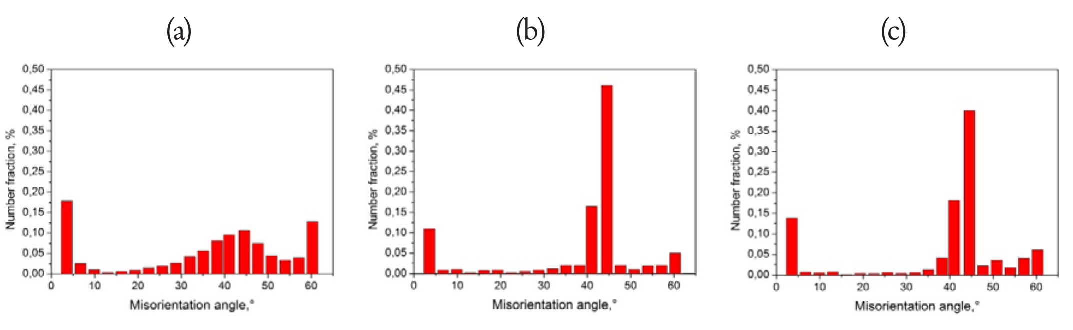

Figure 8. The grain misorientation angle between austenite and ferrite in a) parent metal, b) the HAZ, c) the weld.

The high-angle boundaries are known to be cracking-susceptible boundaries. High-angle boundaries content for both phases was reduced from the parent metal, over the HAZ into the weld, thus if a crack is initiated in the HAZ it cannot then readily propagate into the weld metal via such continuous, cracking-susceptible boundaries. The-high boundaries in austenite were decreased from 70% in parent metal to 52% in the HAZ and 56% in the weld. The low-angle boundaries for which content increased in both phases in the weld metal show the ability to induce slip in neighboring grains thus reducing grain boundary stress and susceptibility for crack initiation.

4. Conclusions

The effects of aging at 650°C on the microstructure of welded joints of lean duplex stainless steel S32101 can be summarized as follows:

1. The welded joint in as-welded condition

shows few Cr_2N nitride precipitates located only in the HAZ. The isothermal heat treatment at 650°C for 15 min causes formation of numerous nitride precipitates, both in the parent metal, as well as in HAZ and the weld area. Increasing aging time at this temperature from 15 to 90 min causes the formation of carbides on the grain boundaries and nitride precipitation inside the ferritic grains in each zone of the welded joint.

2. The EBSD analysis of the welded joint after aging at 650°C for 90 min revealed that ferrite content decreased from 45% in parent metal to 40% in HAZ and 39% in the weld. The higher austenite the content in the weld, closer to equilibrium, the optimal are the mechanical properties of welded joints.
3. Grain size of austenite increased gradually from 7.32 μm in parent metal to 11.99 μm in the HAZ and 13.44 μm in the weld. The ferrite shows the smallest grain size in the HAZ, about 6.91μm, while in parent metal it was close to 9μm and slightly increased in the weld to 9.45 μm. The grain shape aspect ratio of austenite in each zone of studied weld was included in the range between 0.42 to 0.44, while grain shape aspect ratio of ferrite was increased from 0.37, characteristic for parent metal to 0.50 in HAZ and 0.46 in the weld area. The increase of grain shape aspect ratio indicates that grains of both phases become more elongated and they show similar shape in the weld and the HAZ.
4. The orientation relationship between neighboring grains of austenite and ferrite observed from EBSD in the weld metal and the HAZ follows both (K-S) and (N-W) relationship favoring (N-W) orientation relationship. The presence of such relationship between austenite and ferrite in the weld metal together with the decrease of high-angle grain boundaries in both phases in the welded joint can make a contribution to reduction of grain boundary stresses and decrease the susceptibility for crack initiation in the weld metal, thus increasing overall weld metal mechanical properties.

Acknowledements

The authors gratefully acknowledge the financial support from the National Science Centre granted based on the decision number DEC-2011/01/B/ST8/06648.

The authors are grateful to Dr Klaudiusz Gołombek form Silesian University of Technology in Gliwice for his valuable support in SEM micro-structural testing.

References

[1] *Practical guidelines for the fabrication of duplex stainless steels*, 2nd Edn., IMOA, 1999.

[2] Guocai C., Ulf K., John T. and Josefin E., Hyper duplex stainless steel for deep subsea applications, *Stainless steel world*, 2009; March: 27-33.

[3] Duplex stainless steel LDX 2404™, Outokumpu Stainless AB, Avesta Research Centre, 1447EN-GB:2 Centrumtryck AB, Avesta, Sweden. September 2010.

[4] Fang Y.L., Liu Z.Y., Xue W.Y., Song H.M. and Jiang L.Z., Precipitation of Secondary Phases in Lean Duplex Stainless Steel 2101 during Isothermal Ageing, *ISIJ Inter.*, 2010; **50**: 286-293.

[5] Liu H., Johansson P. and Liljas M., Structural Evolution of LDX 2101® (EN 1.4162) During Isothermal Ageing

at 600-850°C, 6th European Stainless Steel Conference, Science and Market, 2008, 10-13 June 2008, Helsinki, Finland.

[6] W. Zhong and Z. L. Wang, *Scanning Microscopy for Nanotechnology Techniques and Applications*, Illy, 399.

[7] V. Kazmiruk, *Scanning Electron Microscopy*, Some Applications of Electron Back Scattering Diffraction (EBSD) in Materials Research, InTech.

[8] Baldo S., Brunelli K., Calliari I., Dabala M., Nordi L. and Zanellato M., Characterization of lean duplex stainless steel, http://www.stainless-steel-world.net

[9] Wei Z., Laizhu J., Jincheng H. and Hongmei S., Effect of ageing on precipitation and impact energy of 2101 economical duplex stainless steel, *Mater. Charact*., 2009; **60**: 50-55.

[10] Holmberg B. and Laren M., Welding and applications of the new lean duplex steel LDX 2101. IIW Annual meeting, 2005, Prague, Czech Republic.

[11] Liu H., Johansson P. and Liljas M. Structural Evolution of LDX 2101® (EN 1.4162) During Isothermal Ageing at 600-850°C. 6th European Stainless Steel Conference, Science and Market, 2008, 10-13 June 2008, Helsinki, Finland.

[12] Hsiehand Ch.Ch. and Wu W., Overview of Intermettalic Sigma (σ) phase precipitation in Stainless Steel, International Scholarly Research Network, *ISRN Metallurgy*, 2012.

[13] Gunn R., *Duplex stainless steels Microstructure, properties and applications*, Abington Publishing, Cambridge, UK.

[14] Herrera C., Ponge D. and Raabe D., Characterization of the Microstructure, Crystallographic Texture and Segregation of an As-cast Duplex Stainless Steel Slab, *Materials Technology*, 2008; **79**: 482-488.

[15] Badji R., Chauveau T. and Bacroix B., Texture, Misorientation and Mechanical Anisotropy in a Deformed Dual Phase Stainless Steel Weld Joint, *Mater. Sci. Eng. A*. In-press.

[16] Alvarez-Armas I., Marinelli M.C., Malarria J.A., Degallaix S. and Armas A.F., Microstructure associated with crack initiation during low-cycle fatigue in a low nitrogen duplex stainless steel, *Inter. J. Fatigue*, 2007; **29**: 758-764.

[17] Karlsson L. and Bhadeshia H.K.D.H., Some European Developments in Welding Consumables, *J. of the Japan Weld. Soc.*, 2011; **80:** 110-119.

[18] Monlevade E.F. and Falleiros I.G.S., Orientation relationships associated with austenite formation from ferrite in a coarse-grained duplex stainless steel, Metall. Mater. Trans. A., 2006; **37**: 939-949.